2017 International Symposium on Lightning Protection (XIV SIPDA), Natal, Brazil, 2nd – 6th October 2017.

Cable shield bonding effectiveness

A tested case with lightning current surge

José Claudio de Oliveira e Silva
APTEMC
São José dos Campos-SP, Brazil
claudio.silva@aptemc.com.br

Celio Fonseca Barbosa
Fundação CPqD
Campinas-SP, Brazil
grcelio@cpqd.com.br

***Abstract*— This paper shows the result of tests with standard 8/20 µs current impulse to evaluate the efficiency on the diversion of lightning surges from cables entering a shielded enclosure, for a few typical cable bonding configurations. A discussion is made about the test results and on the use of a parameter like transfer impedance to characterize cable transits.**

***Keywords*— Earthing, bonding; pigtail, 360 bond; cable shield, cable bonding, cable earthing; lightning protection.**

I. INTRODUCTION

The importance of making proper bonding of cable shields to the metallic wall of an enclosure, when the cable traverse the wall, is still unknown by a large number of professionals working on electrical installations. The shielding efficiency of an enclosure can be seriously degraded by cables that are allowed to carelessly enter the enclosure. While small openings (door slits, display, ventilation, etc) can be made so as to have field penetration under control, the situation involving cables is quite different. By being long and normally exposed to electromagnetic fields, cables pickup and conduct electromagnetic disturbances from the external environment to the internal environment, and vice-versa, increasing the risk of electromagnetic compatibility (EMC) problems.

The subject is not only important at equipment level, but also applies to entire electrical installations, specially if lightning is concerned. As a high intensity transient disturbance, with low to moderately high frequency content (up to a few MHz), the lightning current is the most obvious disturbance source when dealing with lightning problems. Even though (spatial) shielding against lightning electromagnetic impulse (LEMP) is part of the surge protection measures (SPM) [1], the diversion of current away from internal installations is a matter of great attention, since the effects of a small portion of the lightning current near to sensitive equipment can be more important than the effect of full lightning current at larger distances.

The bonding of incoming cables at cable entrances are not only important for solidly shielded enclosures and rooms (e.g. container-like equipment shelters), but also applies to more open shielding topologies such as bonding mats, which are meshes of conductors installed near complex systems as those in telecommunication centers, datacenters and others. Besides offering a path for the unwanted currents, these bonding mats have the function of spreading (diluting) the currents in a wide area, reducing its effects on the protected system. So, the diversion of unwanted currents from cables to these bonding mats, at the point they ingress the protected environment, follows the same principle as for enclosures. The boundary of a volume around which cables are expected to be bonded to the common bonding network (CBN) of the installation, may also define a lightning protection zone (LPZ), as defined in [1].

Shielded cables or waveguides from rooftop or tower-mounted antennae are one of the major threats for installations, since they can bring a significant share of lightning current directly on to the connected and interconnected equipment [2]. In this case, the current comes mostly concentrated on the cable shield. If it is allowed to enter, it flows through the installation causing strong interactions with internal cables and respective interconnected equipment ports. Moreover, lightning current surges are often induced into loops formed by the wiring of an installation [3], [4] and may jeopardize the connected equipment even in the absence of a direct flash to the installation.

Even though well designed radio equipment to which an antenna cable connects can withstand the passage of high intensity surge current through its enclosure, the same cannot be said about interconnected power supply and data equipment, as well as other nearby equipment, and the people operating them as well. Therefore, diverting lightning current surges from cables before they enter the installation is a matter of EMC and safety.

It shall be realized that current diversion from cable shield does not help with the surge that was transferred to the inner circuit of the cable during the current flow along the external portion of the cable. To protect against surges propagating inside the cable, surge protective devices (SPD) are required.

This paper deals with the bonding of a shielded cable at the cable entrance of a shielded enclosure. Tests showing current waveforms are presented, which look very elucidative and convincing about the advantages of a properly made cable bonding.

In section II the considered cable bonding configurations are introduced. In section III the measured effectiveness of the bonding configurations are presented according to the criterion defined therein. A discussion is made in section IV on the test results based on approximate calculations and on a meaningful parameter to characterize the performance of fittings intended

to provide electrical bonding of cables at cable entrances, followed by the conclusions in section V.

II. BONDING CONFIGURATIONS

The 360° bond (also 360° connection or circumferential connection), as in Fig. 1(a), is the one from which the best current diversion performance should be expected, limited only by the performance of the enclosure itself, as the diverted current flows through it. It can be made by welding, feed-through connectors or by some other means that is short and ensure a radial spreading of the disturbing current over the enclosure wall. The advantage of this type of bonding with respect to a pigtail connection, Fig. 1(b), is mentioned or more deeply treated in numerous publications [1], [5]-[13].

In all cases, the bonding configurations do not affect the integrity of the cable shielding significantly[1], since the cable passes through the wall till the equipment it is connected to, but they do affect the shielding integrity of the enclosure.

The basic bonding configurations considered in this paper are based on some configurations found in real installations. They are represented in Fig. 2, as they were realized in the test setup described in the next section. As it can be seen, they go from an extreme to the other, i.e., from no bonding at all (Case 0) to the best 360° bond (Case 4), passing through three intermediate cases: a long connection down to the earth-termination system, via an isolated external earthing bar near the feed-through window (Case 1), a pigtail connection to the shelter wall (Case 2) and a very short connection provided by a commercial sealing and bonding cable transit (Case 3).

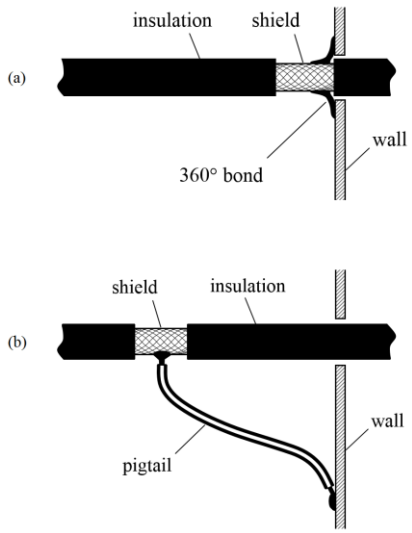

Fig. 1. The 360° bond (a), where the shield is shortly bonded to the enclosure all around its circumference; and the pigtail connection (b), where the connection between cable shield and enclosure is made by a conductor of some lenght; In this representation, the shield is braided.

[1] Regarding the disturbing current, a pigtail connection will provoke a strong non-homogeneity of the current distribution on the shield near such a connection. This will change the inductive component of the cable transfer impedance and may cause an increase of the voltage coupled to the inner circuit of the cable. This effect is probably small in most applications.

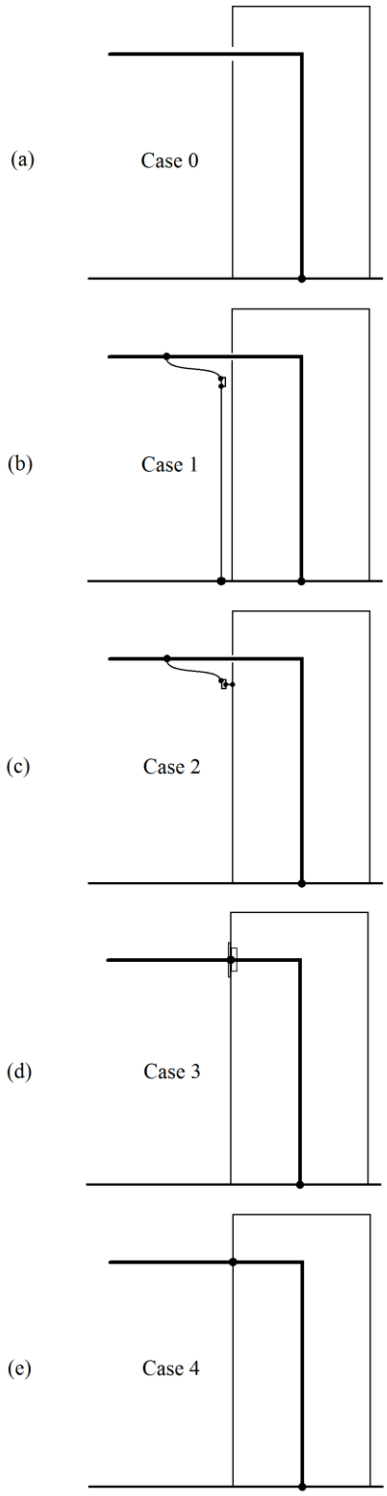

Fig. 2. Bonding configurations, Cases 0 to 4.

The configuration shown in Fig. 2(b), Case 1, is usually seen in mobile telephony radio base stations (RBS) in Brazil, even when the shelters are metallic. Note that [13] recommends similar earthing practice, but for non-metallic shelters.

III. CABLE BONDING EFFICIENCY TESTS

The tests were made by applying 8/20 µs current impulses [14] on the outer conductor of a coaxial cable that enters a shielded enclosure, recording these currents and the currents entering the enclosure, for all bonding configurations as depicted in Fig. 2.

A. *Efficiency definition*

For the purpose of the tests presented here, the bonding efficiency η was defined as the ratio between the current diverted by the cable bonding arrangement and the applied current, Fig. 3.

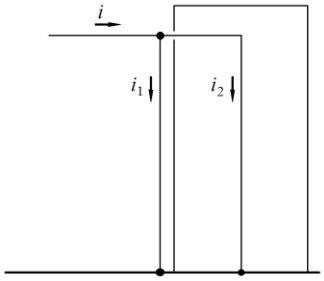

Fig. 3. The applied current i, the diverted current i_1 and the current entering the enclosure i_2 are used to define the efficiency η.

$$\eta = \frac{i_1}{i} = 1 - \frac{i_2}{i} \qquad (1)$$

The measured currents are i and i_2, current peak values. It is clear that ideal results are when $i_1 \to i$ ($i_2 \to 0$) and $\eta \to 1$.

B. *Test Setup*

The enclosure is a shielded cabinet (aluminium, wall thickness 0.8 mm). The cabinet is laid on a metallic ground plane (also aluminium) and connected to it at several points, through which the applied current returns to the generator, Figs. 4 and 5. The ground plane makes the role of earth-termination system.

Fig. 4. General view of the test setup showing the current surge generator, coaxial cable, shielded cabinet, ground plane and digital oscilloscope; The shown configuration corresponds to Case 1, Fig. 2(b).

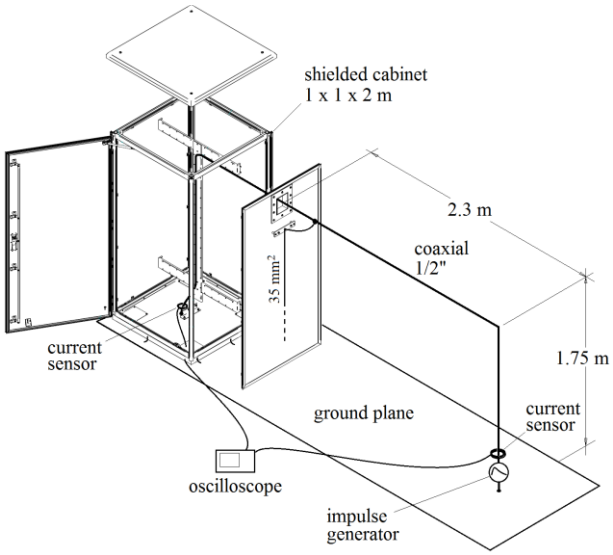

Fig. 5. Test setup with an exploded view of the shielded cabinet; The shown configuration corresponds to Case 1, Fig. 2(b).

The impulse generator injects current on the coaxial cable, which is bonded to the cabinet base, internally (as if it were connected to an internal equipment that is normally bonded to the metallic structure, internally). The current returns to the generator by the metallic ground plane.

The measuring system is composed by an oscilloscope Tektronix TDS 3014B (basic settings: 1 MΩ input impedance; bandwidth (BW) limited at 20 MHz; 10 µs/div.; 10^8 samples/s) and two current sensors type Pearson 110 (5 kA, BW from 1 Hz to 20 MHz).

For test Cases 0, 1 and 2, the coaxial cable passes through isolated modules of the cable transit used in the tests. A description of the bonding configurations follows:

- Case 0: no bonding of the cable shield at the cable entrance.
- Case 1: the outer conductor of the coaxial cable is connected to an external earthing bar located 25 cm below the point the coaxial cable enters the cabinet, which is in turn connected to the ground plane via a straight, 1.5 m long, 35 mm^2 (green) cable. The bar is isolated from the cabinet. The connection between the coaxial cable and the bar used a 0.6 m long, AWG-6 conductor, from a commercial earthing kit for antenna feeders. The connection to the coaxial is 0.5 m away from cabinet wall, see Fig. 4 and Fig. 6(b).
- Case 2: the 35 mm^2 cable is removed and the bar is directly bonded to the cabinet wall by two flat braids. This is the configuration closer to what can be called a "pigtail connection". See Fig. 6(c).
- Case 3: the pigtail is removed and the outer conductor of the coaxial cable is bonded to the cabinet wall via a commercial cable transit (Roxtec BG^{TM}) that provides sealing and cable bonding to its frame, which is attached to the wall. Fig. 6(d).
- Case 4: the coaxial cable is replaced by an ordinary 6 mm^2 conductor which is bonded to an aluminium plate (0.5 mm thick) that replaces the cable transit, being likewise attached to the cabinet wall.

A view of the feed-through window, bonding configurations and the cable inside the cabinet are shown in Fig. 6, 7 and 8.

(a) Feed-through window with braided tape; 0.15 x 0.18 m opening.

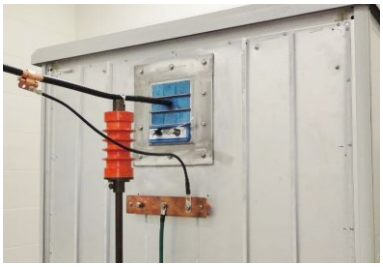

(b) Case 1: Pigtail + 35 mm^2 cable; isolated feed-through modules.

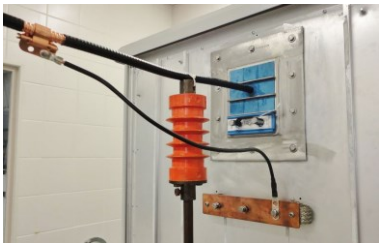

(c) Case 2: Pigtail and copper bar bonded at two ends to cabinet wall.

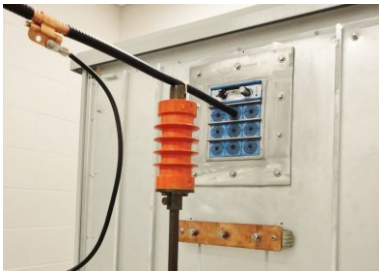

(d) Case 3: Cable shield bonded at cable transit (see Fig. 7).

(e) Case 4: Aluminum plate and 6 mm^2 cable.

Fig. 6. Feed-through window (a) and bonding configurations (b) to (e).

Fig. 7. Sealing and bonding modules of the Roxtec BG^{TM} cable transit used in Case 3; the outer conductor of the coaxial cable makes contact with the frame by means of a meshed arrangement of large and short braids.

Fig. 8. Views of the coaxial cable inside the cabinet; pieces of foam are used to separate the cable from metallic parts; the Pearson current sensor is placed near the base of the cabinet; the braided shield for the current sensor cable is bonded to the cabinet at the point it enters, from below.

The coaxial cable is a Heliax/Commscope ® LDF4-50A, ½-inch nominal size, with outer conductor in corrugated copper. The inner conductor was not used (left open).

C. *Test Results*

The test results are shown in Table I and Figs. 9 and 10.

The efficiency values in Table I are according to (1), taking the peak values of i and i_2 (Fig. 3), for i = 600 A.

The relatively low frequency content of the impulse produced well behaved current waveforms. The applied current was around 600 A in all cases, so that all waveforms in Fig. 9 were normalized to this value for better visualization. The relatively large test setup (see Fig. 5) altered the 8/20 µs current wave shape of the combination wave generator, which became 8/35 µs, approximately (practically the same in all tested cases).

TABLE I. CABLE BONDING MEASURED EFFICIENCIES.

Case	**Peak current (A)** i_2	**Efficiency (%)** $\eta = 1 - \frac{i_2}{i}$
0	600	0
1	225	62.5
2	108	82.0
3	3.63	99.4
4	1.96	99.7

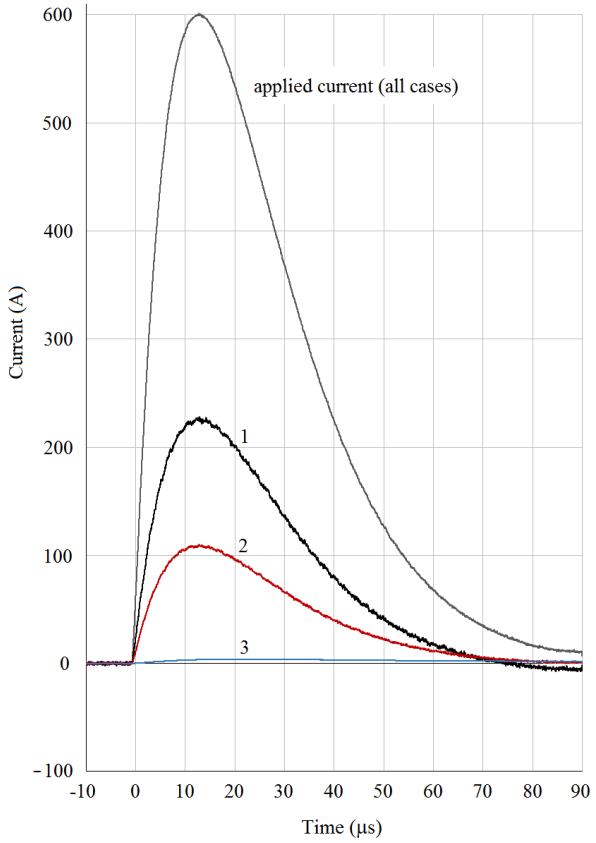

Fig. 9. Applied current (i) and currents penetrating the cabinet (i_2) for Cases 1, 2 and 3, normalized to 600 A; Case 0 coincides with applied current; Case 4 is too close to Case 3, so just Case 3 is shown.

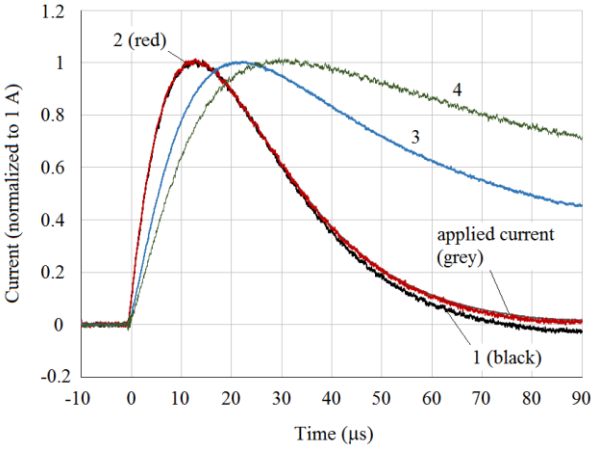

Fig. 10. Currents of Fig. 9, normalized to unity for wave shape comparison.

IV. Calculations and Discussions

A. Modeling the test setup

Some calculations were made to verify if simple impedance expressions could permit addressing the problem of cable bonding for similar configurations and if the enclosure, as well as the cable transit, which are complex elements to deal with, could be represented by simple equivalent impedances, or transfer impedances.

The circuit impedances are represented in Fig. 11. Z_1 and Z_2 denote the self impedances of the external and internal paths, respectively, through which flow i_1 and i_2. In Case 0, $Z_1 = \infty$. In Cases 2, 3 and 4, the cabinet is part of Z_1.

The fields from current i on the circuit between generator and point x are neglected. When current diversion is made at point x, current i_2 is given by (2) and by (3) if made at point y.

$$i_2 = i\,\frac{Z_1 - M_{12}}{Z_1 + Z_2 - 2M_{12}} \tag{2}$$

$$i_2 = i\,\frac{Z_1}{Z_1 + Z_2} \tag{3}$$

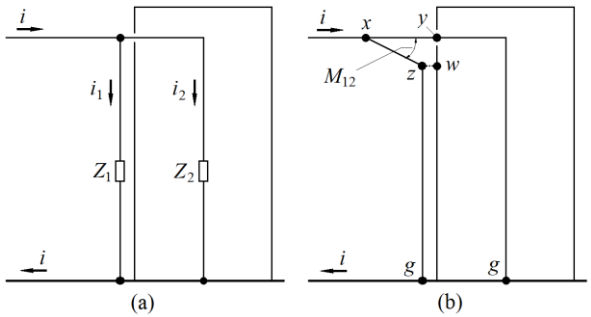

Fig. 11. Circuit impedances; (a) general representation of circuit splitting in two impedances Z_1 and Z_2; (b) definition of circuit segments.

Z_2 is practically given by the impedance of the outer conductor of the coaxial cable, except by a short piece of 6 mm^2 cable used for connection of the coaxial to the cabinet base, see Fig. 8, and the impedance inserted by the current sensor, that is very small. In case 4, Z_2 is the impedance of a 6 mm^2 cable that replaced the coaxial cable all the way from generator to cabinet base. For the relatively slow applied current impulse, skin effect is neglected and all cable impedances are reasonably well represented by their d.c. resistances and external inductances.

The mutual inductance between the vertical portions of Z_1 and Z_2 was arbitrarily omitted. It is difficult to calculate due to the presence of the metallic cabinet surrounding Z_2. It was assumed that the cabinet reduces the mutual inductance between them. On the other hand, the presence of the cabinet was omitted when calculating the inductance of Z_2. The cabinet could be considered, at least partially, as the outer conductor of a larger coaxial system, being the coaxial cable its inner conductor, but this condition was disregarded. It was also an arbitrary decision, although considering the cabinet in any way would also be arbitrary in these calculations. The inductance of the segment zg, Fig. 11(b), was calculated as being the inductance of a conductor over a ground plane (the cabinet wall), taking its short distance to the wall (~ 5 cm). The mutual inductance between segments xy and xz was calculated for several approximate configurations, being adequate to round it to 0.1 μH.

It is obvious that numerical simulations would be necessary for a more precise approach, taking the cabinet into account.

The applied current, Fig. 9, can be well represented by the Heidler function [15], with the following parameters:

$$i(t) = \frac{I}{k} \frac{\left(\frac{t}{T_1}\right)^n}{1+\left(\frac{t}{T_1}\right)^n} e^{\frac{-t}{T_2}} \qquad (4)$$

$I = 600$ A; $k = 0.07786$; $T_1 = 50$ µs; $T_2 = 15$ µs; $n = 11$

The following approximate characteristics are interesting to report:

- Peak value: 600 A
- Wave shape: 8/35 µs
- $di/dt_{max} = 0.1$ kA/µs
- 10 % amplitude of frequency content @ 40 kHz
- 1 % amplitude of frequency content @ 120 kHz

Table II gives the calculated values of resistances and inductances for the circuit segments indicated in Fig. 11(b), for the cabinet not making part of these impedances.

TABLE II. SEGMENTS, RESISTANCES AND INDUCTANCES.

Segment	Length (m)	Resistance (mΩ)	Inductance (µH)	Mutual inductance (µH)
xy	0.50	1.35	0.40	
yg[a]	2.25	6.36	2.39	
yg[b]	2.25	6.95	3.19	
xz	0.61	0.85	0.66	
zg[c]	1.5	0.79	1.02	
xy/*xz*				0.1

a) via coaxial cable inside the cabinet.
b) via 6 mm² cable inside the cabinet (case 4).
c) with *zw* open.

For Case 1, where the currents flow on cables only, i.e. the cabinet does not participate in the circuit in this simplified approach, ($Z_1 = Z_{xz} + Z_{zg}$), the current division calculated by cable impedances was in good agreement with the measurements, see Table III and compare with Table I (0.3 % difference on the efficiency).

For Case 2, where external current path is partially a cable (the pigtail) and partially the cabinet, ($Z_1 \cong Z_{xz} + Z_{wg}$, neglecting Z_{zw}), the current division calculated by cable impedances only was also in good agreement with the measurements. Check the 82.6 % efficiency in Table III (0.6 % difference with the corresponding measured value).

For Cases 3 and 4, where i_1 flows through the cabinet, there was no conditions for determining neither the impedance of the cabinet nor the impedance of the cable bonding to the cabinet, due to complex geometries and current distribution, not to mention additional difficulties such as contact resistances and skin effect. In fact, an attempt was made to calculate Z_1 for Case 4, by considering the spreading resistance on the cabinet wall, from the region of current injection (radial current flow) up to some distance, and assuming zero inductance, but the resulting impedance was too low to permit arriving at a reasonable current division.

TABLE III. CALCULATED EFFICIENCIES.

Case	Peak current i_2 (A)	Efficiency $\eta = 1 - \frac{i_2}{i}$ (%)
0	600	0
1	223.5	62.8
2	104.6	82.6
3	3.56[a]	99.4
4	1.965[b]	99.7

a) Considering $Z_{adj(3)}$.
b) Considering $Z_{adj(4)}$.

The value of Z_1 was then adjusted by try and error, for best matching with the measurements, assuming it could be represented by an RL series impedance. An important feature to observe about measured current i_2 in Cases 3 and 4, is their wave shapes that differ from the other currents, see Fig. 10.

The peak currents and efficiencies were then accommodated to values in good agreement with measurements, as it can be seen in Table III, by assigning the following impedances to the cabinet (that includes the cable transit in Case 3):

$Z_{adj(3)} = 0.35$ mΩ + 10 nH (adjusted Z_1 for Case 3)

$Z_{adj(4)} = 0.28$ mΩ + 6 nH (adjusted Z_1 for Case 4)

The calculated current waves are shown in Fig. 12 and 13, for direct comparison with the measured values. For Cases 3 and 4, the peak current and efficiency values in Table III could be adjusted to be very close to the measured values.

The impedances $Z_{adj(3)}$ and $Z_{adj(4)}$ allowed a good agreement between the current waves up to their peaks, but the wave tails decay slower than the measured ones, see Fig. 13, Cases 3 and 4. A later analysis (with the test setup disassembled but some components still available) indicated that the impedance of the inner circuit (Z_2) was underestimated. Some contact resistances could not have been neglected, what would make the calculated waves in Cases 3 and 4 to decay faster. It is worth mentioning that i_2 wave shapes (cases 3 and 4) depend mostly on the internal circuit Z_2, as $Z_2 >> Z_1$.

The difference between the two adjusted impedances in (5) gives the impedance inserted into Z_1 path by the cable transit used in the test (Case 3), with due reservations to the limitations of this simplified approach. This impedance can be called as a transfer impedance of the cable transit, Z_T:

$$Z_T = Z_{adj(3)} - Z_{adj(4)}, \qquad (5)$$

that in this case is $Z_T = 0.07$ mΩ + 4 nH.

B. Transfer impedance of cable transits

An useful practical experience gained from these tests and calculations is that the performance in the lightning current diversion provided by a given shielded enclosure, combined with a given cable transit, can be estimated by adding the transfer impedances of these two parts.

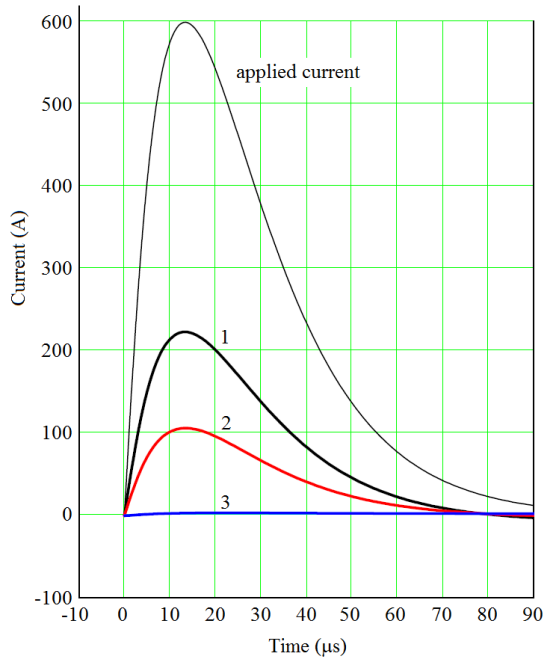

Fig. 12. Calculated currents for Cases 1, 2 and 3; Applied current according to (4) and given parameters.

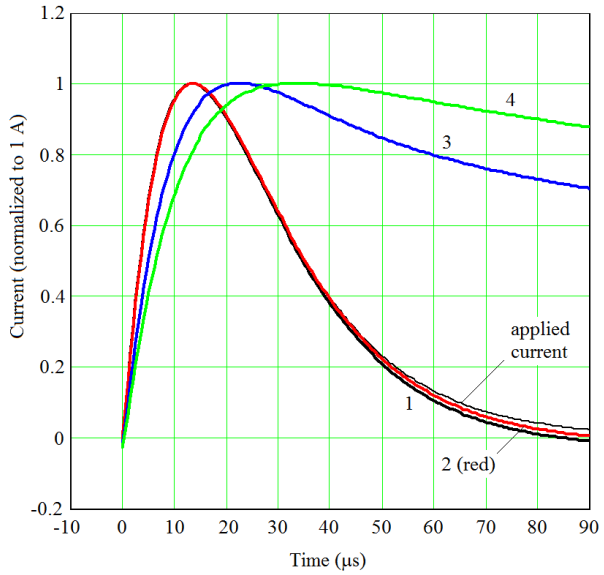

Fig. 13. Currents of Fig. 9 normalized to unity for wave shape comparison.

The transfer impedance of a shielded enclosure can be determined by measurement. The simplest way could be by measuring the d.c. resistance between cable entrance and the earthing terminal(s) of the enclosure, and the transfer inductance could be measured at one or more frequencies, taking into account the entire loop that the cable is expected to form inside the enclosure.

There is a frequency limit associated with the size of the loop, of course, but for lightning frequencies (up to a few MHz) a couple of meters should not be a problem. Regarding skin effect, excepting for unusually thick walls, the estimation will be conservative if it is neglected. Considerations shall also be made about the external current circuit, since it will affect the current distribution over the enclosure, affecting the transfer impedance.

The discussion above leads one to consider what would be a meaningful transfer impedance of a cable transit, to be used in association with the transfer impedance of an enclosure, specially if it is provided by the manufacturer. The resistive component of the transfer impedance is not a problem, but the inductive component, concerning the inductance of the bonding path(s) of the cable transit, should be measured (on the receiver side, Fig. 14) in a defined enclosure, along a circuit bounding a certain loop area, in a way that it would provide a more realistic parameter. A preliminary suggestion is presented in Fig. 14 for transfer impedance measurement in frequency domain.

The bonding path indicated in Fig. 14 represents the impedance along which the transferred voltage, to be measured, is developed. The current is applied by a generator in a coaxial structure, so it does not affect the voltage inside the shielded box and practically no current flows on it, since it is isolated and the common-mode (CM) voltage at the box is reduced due to the coaxial feeding structure. The connection box, small sized, provides the transition from the coaxial structure (from generator) to the cable transit. A thick contact plate, which can belong to the connection box, prevents any appreciable voltage to appear on the internal surface of the shielded box. The isolation shall have low capacitance for minimum capacitive current return.

The shielded box is part of the voltage measuring circuit, dimensioned for embracing a reasonable amount of magnetic flux generated by the bonding path(s), since it is important in terms of the efficiency of current diversion. It should be sized based on two main parameters: the size of the cable transit, i.e. the length of bonding path, and the maximum measuring frequency.

For being able to capture at least 50 % of the total flux generated by the current flowing on the bonding path, the shielded box sides should be at least 10 times longer than the bonding path. On the other hand, the box should be electrically small for proper use of inductance concept, so that it should have dimensions not longer than one-tenth of the wavelength ($\lambda/10$) related to the maximum measuring frequency. For bonding paths up to 10 cm and frequency up to 30 MHz, a 1-m side cube is appropriate.

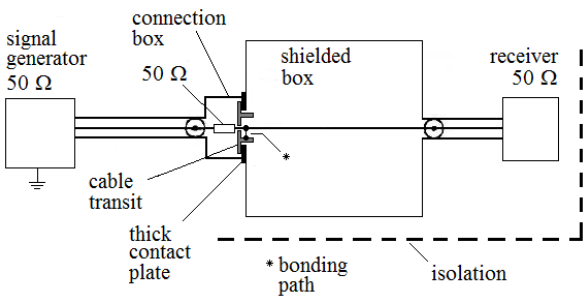

Fig. 14. Suggested test setup for cable transit transfer impedance measurement.

From the test setup suggested in Fig. 14, the transfer impedance Z_T, in Ω, is given by:

$$Z_T = 50 \frac{V_r}{V_g} \quad (6)$$

where V_r and V_g are the generator output voltage and receiver voltage, respectively.

The efficiency η as defined by (1) is given by:

$$\eta = 1 - \frac{V_r}{V_g} \quad (7)$$

Note that V_r depends on the dimensions of the shielded box, so that they should be standardized in order to compare the transfer impedance values from different cable transits.

V. CONCLUSION

The test results are technically sound and provide a convincing argument for professionals involved with electrical installations, particularly with lightning protection. The figures in Table I and, specially the current curves in Fig. 9, demonstrate in a clear way the importance of making a proper bonding of cable shields at entrances of shielded enclosures.

A metallic enclosure naturally offers a high level of shielding for equipment against the radiated effects of lightning. It also provides excellent conditions for lightning current diversion for it is an electrically continuous, enclosing structure. It is therefore wise to consider that these inherently good qualities of metallic enclosures are not wasted by a badly done cable bonding.

Current diversion by means of cables, e.g. pigtails and/or relatively long earthing conductors, can be estimated by their inductances only. Estimation of current diversion via shielded enclosures is more involving. The current diversion efficiency defined in this paper, for lightning, proved to be relatively easy and good enough to evaluate the effectiveness of cable bonding at cable entrances.

A standard method for measuring transfer impedance of cable transits, that gives a clear meaning to it and make it possible to use in the design of shielded enclosures or rooms is suggested.

ACKNOWLEDGMENTS

The authors would like to thank Roxtec Latin America Ltda (Brazil) and Roxtec International AB (Sweden) for the interest and support for the realization of this study and tests. The valuable advices and discussions with Antônio Roberto Panicali are also very much appreciated.

REFERENCES

[1] IEC 62305-4, “Protection against lightning – Part 4: Electrical and electronic systems within structures”, Ed. 2.0, 2010.

[2] C. F. Barbosa, F. E. Nalli, S. Person, and A. Zeddam, “Current distribution in a telecommunication tower struck by rocket-triggered lightning”, *IX Int. Symp. on Lightning Protection*, Foz do Iguaçu, Brazil, 2007.

[3] C. F. Barbosa and J. O. S. Paulino, "A closed expression for the lightning induced voltage in short loops", *IEEE Trans. on Electromagnetic Compatibility*, vol. 58, pp. 172-179, 2015.

[4] J. O. S. Paulino, P. Assunção, and C. F. Barbosa, "Lightning induced voltages in large loops", *XIII Int. Symp. on Lightning Protection*, 2015, Balneário Camboriú, vol. 1. pp. 1-7, 2015.

[5] H. W. Ott, “Noise reduction techniques in electronic systems”, John Wiley & Sons, 1976.

[6] J. Goedbloed, “Electromagnetic compatibility”, Prentice Hall, 1990.

[7] C. R. Paul, “Introduction to electromagnetic compatibility”, John Wiley & Sons, 1992.

[8] P. Degauque, J. Hamelin, “Electromagnetic compatibility”, Oxford University Press, 1993.

[9] A. Tsaliovich, “Cable shielding for electromagnetic compatibility”, Van Nortrand Reinhold, 1995.

[10] F. M. Tesche, M. V. Ianoz, T. Karlsson, “EMC analysis methods and computational methods”, John Wiley & Sons, 1997.

[11] Guide 124, “Guide on EMC in power plants and substations”, CIGRÉ, 1997.

[12] IEC TR 61000-5-2, “Electromagnetic compatibility – Part 5: Installation and mitigation guidelines – Section 2: Earthing and cabling”, IEC, Ed. 1, 1997.

[13] ITU-T K.56; “Series K: Protection against interference – Protection of radio base stations against lightning discharges”, ITU-T, 2010.

[14] IEC 61000-4-5, “Electromagnetic compatibility (EMC) – Part 4-5: Testing and measurement techniques – Surge immunity test”, Ed. 2.0, 2015.

[15] F. Heidler, “Analitsche blitzstromfunktion zur LEMP-berechnung”, *Proc. of 18th Int. Conf. on Lightning Protection*, Munich, Germany, 2–9 Aug. 1985.